

Supporting Information

Air-Stable Plasmonic Bubbles as a Versatile Three-Dimensional Surface-Enhanced Raman Scattering Platform for Bi-Directional Sensing of Gaseous Analytes

Yong Xiang Leong^a, Charlynn Sher Lin Koh^a, Gia Chuong Phan-Quang^a, Emily Xi Tan^a, Zhao Cai Wong^a, Wee Liang Yew^a, Bao Ying Natalie Lim^a, Xuemei Han^a, Xing Yi Ling^{a*}

^a Division of Chemistry and Biological Chemistry, School of Physical and Mathematical Sciences, Nanyang Technological University, Singapore 637371.

*Email: xyling@ntu.edu.sg

Materials and Methods

Chemicals. Silver nitrate (AgNO_3 , $\geq 99\%$), anhydrous 1,5-pentanediol (PD, $\geq 97\%$), poly(vinylpyrrolidone) (PVP; average $M_w = 55,000$), 1H,1H,2H,2H-perfluorodecanethiol (PFDT, $\geq 97\%$), sodium dodecyl sulfate (SDS, $\geq 98.5\%$), glycerol ($\geq 99.5\%$), methylene blue (MB, $\geq 82\%$) and 4-methylbenzenethiol (MBT, $\geq 98\%$) were purchased from Sigma Aldrich. Copper (II) chloride (CuCl_2 , $\geq 98\%$) was purchased from Alfa Assar. Gellan gum was purchased from CP Kelco. Ethanol (ACS, ISO, Reag. Ph Eur) was purchased from Fischer Chemical. 2-propanol (IPA, $\geq 99.7\%$) was purchased from J. T. Baker., Avantor® inc. Thermo Scientific QSP 1 – 200 μL pipette tips were purchased from Fischer Scientific. Milli-Q water ($> 18.0 \text{ M}\Omega \cdot \text{cm}$) was purified with a Sartorius Arium® 611 UV ultrapure water system. All chemicals were used without further purification.

Synthesis and Purification of Ag nanocubes. Ag nanocubes were synthesized in high yield using the polyol reduction method.¹ In separate vials, 10 mL of PVP (20 mg/mL), AgNO_3 (20 mg/mL) and CuCl_2 (8 mg/mL) were dissolved in PD. 35 μL of the CuCl_2 solution was added to the AgNO_3 solution and mixed well. Thereafter, 20 mL of PD was heated to 190 °C for 10 min. Aliquots of 250 μL of PVP and 500 μL of AgNO_3 solutions were then added in alternation to the reaction flask until the reaction mixture turned reddish-brown. The reaction mixture was repeatedly washed by ethanol and centrifuged before being subjected to vacuum filtration using polyvinylidene fluoride filter membranes (Durapore®) with pore sizes 5 μm , 0.65 μm , 0.45 μm and 0.22 μm to remove impurities.

Surface functionalization with PFDT. The filtered nanocube solution (1 mL) was added to IPA (1 mL) while stirring. PFDT solution (10 mM, 240 μL) was then added dropwise to the mixture and stirred for 3 h. The mixture was washed with ethanol twice before dispersing into a 1:1 ethanol/IPA (1 mL) mixture. PFDT solution (10 mM, 250 μL) was added dropwise to the mixture and stirred for another 3 h. The resultant mixture was washed with 1:1 ethanol/IPA for three times and re-dispersed in a 1:1 ethanol/IPA solution.

Preparation of bubble gel. SDS (20 mg), gellan gum (20 mg), glycerol (0.1 mL) and water (0.4 mL) were mixed in a 20 mL vial with stirring at 80 °C. PFDT-functionalized Ag nanocubes (5 mg, 20 mg, 100 mg, 250 mg) were dispersed in water (0.5 mL) and added to the stirring mixture dropwise. The bubble solution was then left to cool in room temperature and harden to gel form.

Fabrication of Plasmonic bubbles. The bubble gel was heated to 80 °C to convert the gel into solution form. A 1 – 200 μL QSP pipette tip was inverted and dipped into the mixture to create a thin bubble film across the larger opening. For characterization of our Plasmonic bubble with MB, MB was added to the gel mixture before gently passing approximately 1 cm^3 of N_2 through the smaller opening to create the Plasmonic bubble. The as-formed Plasmonic bubble is left to stabilize for 10 minutes prior to SERS measurements. For analysis using MBT in the first mode (internal), excess solid MBT were placed in a 1 mL syringe attached with a 1 – 200 μL QSP pipette tip. Once the internal volume of the syringe was saturated with MBT vapor, the pipette tip was inverted and dipped into the mixture to create a thin bubble film across the larger opening. The syringe pump is then pushed to introduce approximately 1 cm^3 of MBT into the formed Plasmonic bubble. For analysis using MBT in the second mode (external), the as-formed Plasmonic bubble using N_2 is incubated in an enclosed Raman cell containing excess solid MBT. In both cases, the smaller opening of the pipette tip was then sealed with parafilm to prevent bubble shrinkage and SERS measurements were conducted about 1 minute after Plasmonic bubble formation due to the inevitable delay between the bubble formation and SERS measurements in practice.

SEM Characterization. SEM imaging was performed using a JEOL-JSM-7600F microscope at an accelerating voltage of 5 kV. Prior to SEM imaging, the Plasmonic bubble is frozen with liquid nitrogen and broken into small pieces. A piece of solid bubble film was fixed onto the SEM sample holder using carbon tape for imaging of the bubble surface. The same piece was then broken into halves and subject to cross-sectional SEM to image the bubble film cross-section.

SERS Measurements. SERS measurements were performed using x-y and x-z imaging modes of the Ramantouch microspectrometer (Nanophoton Inc., Osaka, Japan) with a 532 nm excitation laser (power = 0.06 mW). A 50× (N.A. = 0.55) objective lens was used with 60 s acquisition time for data collection. All SERS spectra were obtained by averaging at least 10 individual SERS spectra within the SERS image.

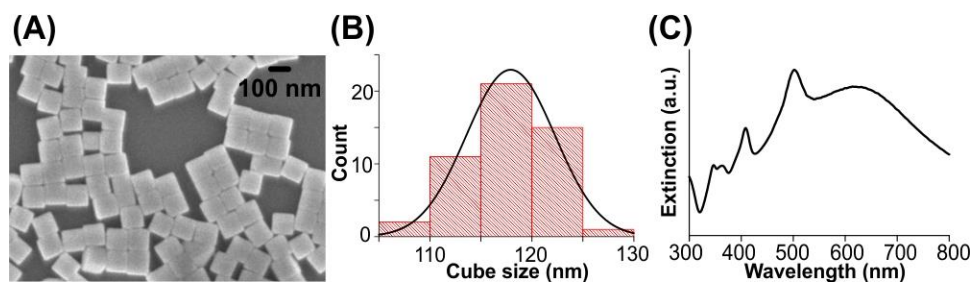


Figure S1. Synthesis and characterization of Ag nanocubes. (A) SEM image of the synthesized Ag nanocubes. (B) Edge length distribution of the nanocubes, which is 117 ± 6 nm. (C) UV-vis extinction spectrum of colloidal Ag in ethanol. The peaks at 355, 408, 501 and 622 nm can be assigned to octupole (355 nm), quadrupole (408, 501 nm) and dipole (622 nm) resonances.²

Table S1. Average bubble lifetime with varying concentrations of gellan gum and SDS. A dash ‘-’ indicates that the bubble bursted during expansion while a cross ‘×’ indicates that the condition has not been tested.

	0% w/v gellan gum	0.5% w/v gellan gum	1% w/v gellan gum	2% w/v gellan gum
0% w/v SDS	-	-	-	-
0.5% w/v SDS	33 s	31 s	×	×
1% w/v SDS	39 s	×	56 s	×
2% w/v SDS	137 s	×	×	7 days

From Table S1, we note that the bubble cannot be formed without adding SDS. This shows that the presence of an amphiphilic moiety is important for the formation of a thin aqueous bubble film. In the absence of gellan gum, the increase in SDS concentration increases the relative bubble stability from 33 s to 137 s. This is because the relative concentration of SDS has not reached its critical value, therefore allowing further decrease in surface tension of the aqueous layer as SDS concentration increases to achieve enhanced bubble stability.

We further investigate the effects of increasing the amount of SDS and gellan gum in a 1:1 ratio. A 1:1 ratio is adopted because excess SDS affects gellan helix formation while excess gellan gum hinders the ability of SDS to stabilize the bubble film.³ Notably, a 2% w/v of SDS and gellan gum is the minimum amount that enables significant stabilization of the Plasmonic bubble film, and hence was adopted for our experiments.

Table S2. Thickness of the Plasmonic bubble film and its standard deviation. The film thickness is an averaged measurement of 5 different Plasmonic bubbles.

Ag nanocube concentration (mg/mL)	Film thickness (μm)	Film standard deviation (μm)
0	16.0	0.3
5	16.9	0.4
20	16.7	0.6
100	16.3	0.3
250	16.6	0.4
Average	16.5	0.5

Supplementary note 1. Calculation of the Ag nanocube occupancy within the Plasmonic bubble film.

From SEM images, we establish that a Ag nanocube has an average edge length of 117 nm (0.117 μm).

Hence, the surface area of 1 Ag nanocube is given by:

$$\begin{aligned}\text{Surface area of 1 Ag nanocube} &= (0.117 \mu\text{m})^2 \\ &= 0.0137 \mu\text{m}^2\end{aligned}$$

At an added Ag concentration of 250 mg/mL, the number of Ag nanocubes in a $1 \mu\text{m} \times 1 \mu\text{m}$ area is estimated to be 58 particles/ μm^2 . The surface coverage is hence calculated to be:

$$\begin{aligned}\text{Surface coverage} &= \frac{58 \times 0.0137 \mu\text{m}^2}{1 \mu\text{m}^2} \times 100\% \\ &= \mathbf{79\%}\end{aligned}$$

Supplementary note 2. Calculation of analytical enhancement factors.

The analytical enhancement factors were calculated using the 1633 cm^{-1} peak of methylene blue, which is indexed to the aromatic C=C stretching vibrational mode.

$$\text{Analytical Enhancement Factor} = \frac{I_{\text{SERS}}}{I_{\text{Raman}}} \times \frac{C_{\text{Raman}}}{C_{\text{SERS}}}$$

where C_{Raman} and C_{SERS} refers to the concentration of methylene blue in the normal Raman and SERS measurements respectively, and I_{Raman} and I_{SERS} refers to the peak signal intensity in the absence and presence of our Plasmonic bubble.

Plasmonic bubble

$$\begin{aligned} \text{Analytical Enhancement Factor} &= \frac{27.4}{0.111} \times \frac{10^{-2}}{10^{-10}} \\ &= \mathbf{2.5 \times 10^{10}} \end{aligned}$$

Supplementary note 3. Elaboration on the sigmoidal relationship between the MB concentration and SERS signal intensity.

At high concentrations of MB (10^{-3} to 10^{-4} M), the aqueous film is highly saturated with MB and the signal intensity is limited by the analytical enhancement provided by the inter-particle plasmonic coupling between Ag nanocubes (Figure 3C). Since the nanoparticle packing density is constant, a decrease in MB concentration will bring about a less than proportionate decrease in the SERS signal intensity. At MB concentrations between 10^{-5} to 10^{-7} M, the observed relationship is approximately linear as the amount of MB in the laser irradiated volume decreases proportionally with the MB concentration. However, at low concentrations of MB (10^{-8} to 10^{-10} M), the SERS signal intensity is determined by the amount of randomly distributed MB, which fall within the laser irradiated volume. Due to the strong inter-particle plasmonic coupling, we observe a less than proportionate decrease in the SERS signal intensity despite a decrease in MB concentration.

References

1. A. Tao, P. Sinsersuksakul, P. Yang, *Angew. Chem. Int. Ed.*, 2006, **45** (28), 4597-4601.
2. Y. X. Leong, Y. H. Lee, C. S. L. Koh, G. C. Phan-Quang, X. Han, I. Y. Phang, X. Y. Ling, *Nano Lett.*, 2021, **21** (6), 2642-2649.
3. V. I. Chizhik, A. A. Khripov, K. Nishinari, *J. Mol. Liq.*, 2003, **106** (2), 249-255.